Hydrology and Earth System Sciences, 7(6), *833–847* (2003) © EGU

Hydrology & Earth System Sciences

Modelling floods in the Ammer catchment: limitations and challenges with a coupled meteo-hydrological model approach

R. Ludwig[1], S. Taschner[2] and W. Mauser[1]

[1]University of Munich, Department of Earth and Environmental Sciences, Luisenstrasse 37, D-80333 Munich, Germany
[2]Università degli Studi di Brescia, Dipartimento di Ingegneria Civile, Via Branze 38, I-25123 Brescia, Italy

Email for corresponding author: ralf.ludwig@lmu.de

Abstract

Numerous applications of hydrological models have shown their capability to simulate hydrological processes with a reasonable degree of certainty. For flood modelling, the quality of precipitation data — the key input parameter — is very important but often remains questionable. This paper presents a critical review of experience in the EU-funded RAPHAEL project. Different meteorological data sources were evaluated to assess their applicability for flood modelling and forecasting in the Bavarian pre-alpine catchment of the Ammer river (709 km²), for which the hydrological aspects of runoff production are described as well as the complex nature of floods. Apart from conventional rain gauge data, forecasts from several Numerical Weather Prediction Models (NWP) as well as rain radar data are examined, scaled and applied within the framework of a GIS-structured and physically based hydrological model. Multi-scenario results are compared and analysed. The synergetic approach leads to promising results under certain meteorological conditions but emphasises various drawbacks. At present, NWPs are the only source of rainfall forecasts (up to 96 hours) with large spatial coverage and high temporal resolution. On the other hand, the coarse spatial resolution of NWP grids cannot yet address, adequately, the heterogeneous structures of orographic rainfields in complex convective situations; hence, a major downscaling problem for mountain catchment applications is introduced. As shown for two selected Ammer flood events, a high variability in prediction accuracy has still to be accepted at present. Sensitivity analysis of both meteo-data input and hydrological model performance in terms of process description are discussed, drawing positive conclusions for future applications of an advanced meteo-hydro model synergy.

Keywords: RAPHAEL, modelling, forecasting, model coupling, PROMET-D, TOPMODEL

Introduction

The remarkable increase in extreme flood events in recent years has led to an urgent social and economic demand for improved prediction and sustainable prevention. Remedial measures require reliable information on the characteristics of floods and on the temporal evolution and spatial extent of runoff volume and peak, which can be investigated by sophisticated simulation techniques.

One of the major tasks in flood hydrology is to link recent progress in atmospheric and hydrological sciences to improvements in real-time flood forecasting. The objective of the EU-funded project RAPHAEL (Runoff and Atmospheric Processes for flood HAzard forEcasting and controL) was to develop advanced methods for forecasting rainfall and related flood events in complex mountain basins (Bacchi and Ranzi, 2003), so as to improve early warning systems. Due to the high frequency of flood events related to different physiogeographic and meteorological aspects, the Ammer basin (709 km²) was selected as a representative catchment of the northern Alps and their forelands, to investigate the manifold features of flood situations in the framework of a one-way coupled atmospheric-hydrological model synergy. This study analysed the available meteorological data sources, processed the data for applications at the catchment scale and evaluated and interpreted the accuracy and reliability of the precipitation data sources available for hydrological flood modelling and forecasting.

Rainfall-runoff models consider catchments as dynamic systems, in which the independent variable, precipitation,

is transferred to the dependent variables evapotranspiration and discharge. These systems are self contained entities of physical parameters that relate the input and output to a certain time increment. Many processes are thereby involved, such as interception, soil saturation or snow accumulation and melt. The complexity of the models used for hydrological simulations depends on the process under consideration, the purpose of the model application, the character of the modelled system and the degree of causality between different variables. Hydrological models range from purely statistical, lumped or distributed conceptual type models to physically-based distributed models. The simulation of storm events or even their forecast demands an accurate comprehension of catchment characteristics, a precise determination of each catchment's flood-related initial boundary conditions and a reliable provision of system input, i.e. precipitation and snowmelt producing runoff. In this study, precipitation data are obtained from Numerical Weather Prediction Models, rain-radar interpretation and rain gauge recordings. These multi-sources of information are used to drive a physically-based and distributed hydrological model framework. Model results are compared with measured precipitation and runoff to evaluate the accuracy and performance of forecast precipitation inputs.

Study area

The Ammer catchment, located south-west of Munich in the Bavarian alpine forelands, covers an area of 709 km² to the catchment outlet at the gauge at Fischen (Fig. 1). It is characterised by physiographic heterogeneity in terms of geology, pedology and land use. From the steep mountainous regions of the Bavarian Alps (> 2100 m asl) the Ammer river heads north through the smoothly reliefed molassic structures of the alpine foreland, before entering Lake Ammer (533 m asl). About 50% of the catchment is forested, while the rest is mainly agricultural (90% pasture, 10% crop). Meteorological measurements indicate a N – S gradient of decreasing temperature and increasing precipitation. Mean annual precipitation is 1200 mm, ranging from 900 mm in the north to over 1800 mm in the mountains.

In the Ammer river, the mean annual streamflow of 16.6 $m^3 s^{-1}$ averages a pluvio-nival runoff regime, in which maximum flow rates result from a transition of snow melt periods in spring to summer precipitation maxima. Floods occur frequently and are usually dominated by saturation excess overland flow due to the poor storage capacities of alpine soils and the high water tables in the northern valley parts of the catchment. The relatively small basin size, coupled with steep slopes, leads to short runoff concentration

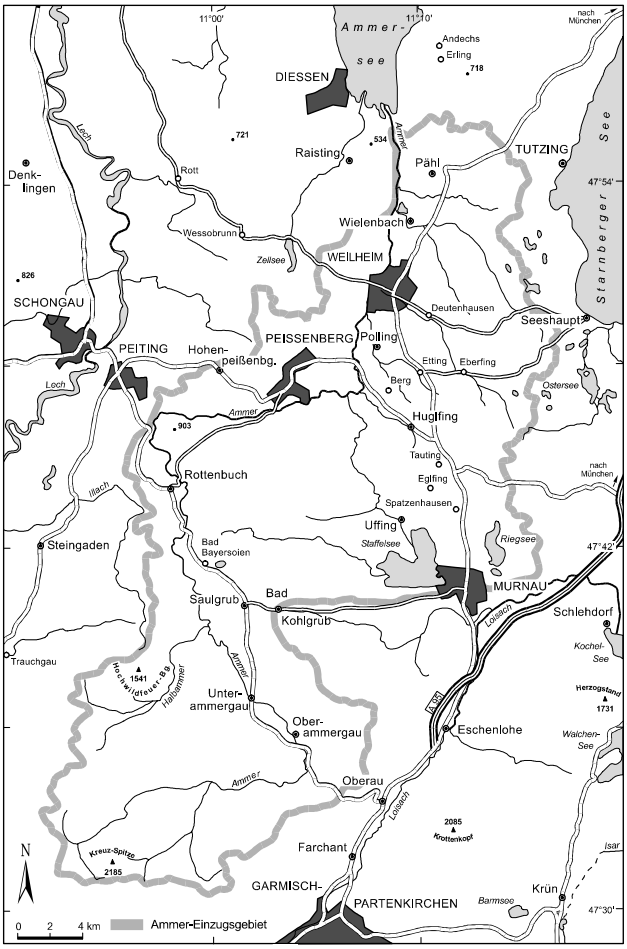

Fig. 1. *The Ammer catchment*

times; consequently, high but temporarily short peak flows result. The ten most severe floods in the past sixty years occurred between early May (caused by overlapping snowmelt and rainfall, peak flow ~ 600 $m^3 s^{-1}$ in 1999) and late August (rainfall only, peak flow ~350 $m^3 s^{-1}$ in 1970).

The model framework

The catchment hydrology of the Ammer catchment is modelled using PROMET-D (PRocess-Oriented Model for EvapoTranspiration and Discharge: Ludwig and Mauser, 2000), a model link established between the physically based SVAT scheme PROMET (Mauser and Schädlich, 1998) and an enhanced distributed GIS-version of the conceptual rainfall-runoff model TOPMODEL (TOPographic MODEL, Beven *et al.*, 1995). PROMET provides the terms of continuous hourly water balance calculations (e.g. evapotranspiration, snowmelt, interpolation of meteorological fields, soil moisture). Upon request, these data are used to drive and/or initialise the conceptual rainfall-

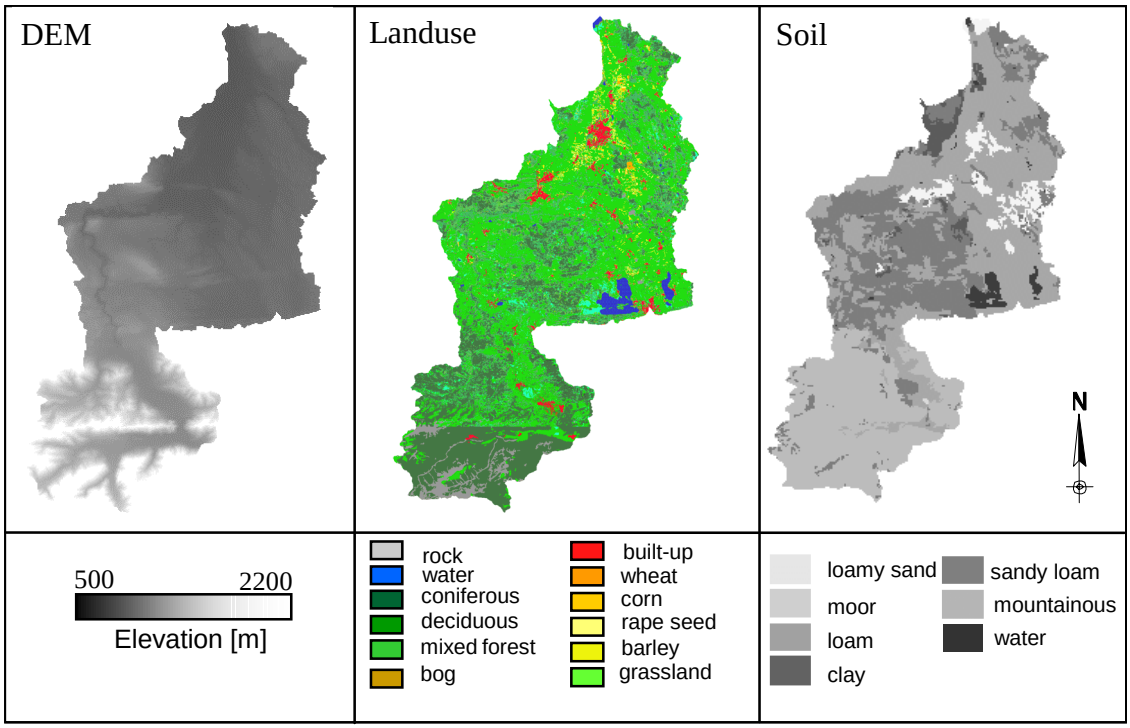

Fig. 2. *Land use, topography and soil types of the Ammer catchment*

runoff model to determine catchment runoff. Note that the concepts and physics behind the two model approaches are significantly different. However, great benefit can be drawn from the validated physically based SVAT-scheme PROMET (Mauser and Schädlich 1998; Strasser and Mauser 2001; Ludwig and Mauser 2000) by providing spatially distributed information on water fluxes, comprising catchment characteristics (e.g. land use, soil, radiation balance), which are seldomly considered in detail for rainfall-runoff modelling. The necessary adaptation of the GIS-based TOPMODEL-version is briefly described later. Both models are performed in hourly time steps on a 100 × 100 m grid resolution. Static input data include land use information (derived from a fuzzy logic based classification of Landsat-TM imagery (Stolz *et al*., 1999)), topography (elevation, slope and aspect derived from a Digital Elevation Model) and the distribution of soil types derived from the Bavarian Bodengütekarte (soil quality map) (Fig. 2). Data tables on soil physics (pore size distribution, porosity, bubbling pressure head and hydraulic conductivity taken from the literature (Brooks and Corey, 1964)) and on plant physiology (leaf area index, albedo, plant height, rooting depth) are assigned to the grids of soil and land use, providing information on the static and dynamic characteristics of the respective objects. The meteorological inputs required to run the SVAT component are precipitation, humidity, temperature, wind and radiation. The following paragraphs describe the basic principles of the model framework. A detailed description of the model setup and its individual components is given by Ludwig and Mauser (2000).

THE SVAT MODEL PROMET

The water balance model PROMET calculates the spatial and temporal variability of evapotranspiration, soil moisture, ground water recharge and snow water equivalent. The PROMET kernel comprises a number of interdependent components delivering the inputs for the Penman-Monteith equation, which combines the energy-balance of the land surface with plant species-dependent surface resistances for water-vapour release. The required modules are:

- a radiation module to calculate the radiation balance for each grid cell according to topography, sun angle and cloud cover (Mauser, 1989);
- a one-dimensional soil water module to model the soil water content as a function of infiltration, exfiltration and capillary rise, applying a simplified solution of the Richards equation (Eagleson, 1978);
- a plant-physiological module;
- modelling the diffusion of transpired water vapour into the atmosphere (Monteith, 1978) ;
- an aerodynamic component modelling the diffusion of

transpired water vapour into the atmosphere (Monteith, 1978);
- a one-layer snow module describing the accumulation and melt processes and calculating the melt water runoff according to energy balance terms (Todini, 1996).

THE EXTENDED TOPMODEL

The extended GIS-based TOPMODEL is computed in a distributed manner (i.e. cell by cell on a 100 grid). While it is based on the principal ideas of TOPMODEL and its distribution function approach, the balancing of the soil root zone is driven by the spatially distributed outputs of PROMET (i.e. actual evapotranspiration, snowmelt, interpolated rainfall). While the approach presented promotes the 'lumped' or 'semi-distributed' TOPMODEL to a 'distributed' version, the basic assumptions underpinning the TOP-MODEL concept (Beven *et al*., 1995; Franchini *et al*., 1996) still need to be held:

- the dynamics of the saturated zone is approximated by successive steady states;
- the hydraulic gradient of the saturated zone is approximated by the local surface slope;
- the decay of hydraulic conductivity with depth is an exponential function of soil storage deficit.

Saturation excess and return flow is calculated by introducing a temporally and spatially dynamic topographic index. The static distribution of index-values used formerly is replaced by a dynamic course of distributed index values representing the seasonal course of saturation excess runoff potential in the catchment. It was found in an earlier study (Ludwig and Mauser, 2000), that the separation of peak flow and baseflow leads to antidromic results in the Ammer catchment when a static distribution of the topographic index is assumed in time, i.e. while the runoff volume is determined correctly, an overestimation of peak flow is discovered during the summer months and vice versa. The extended approach takes into account the variability of plant activity by means of transpiration, rooting and surface roughness and its influence on the variable contributing area to surface runoff. The evapotranspiration-soil-topographic index a_{ET} is calculated by Eqn. (1), where A is the upslope area per unit contour length, K_s is the local saturated hydraulic conductivity and tan b is the local surface slope. ET_c is a dynamic evapotranspiration coefficient, which describes a spatially distributed 'seasonal evapo-transpiration regime' for each pixel through dividing its monthly mean of daily evapotranspiration by its annual daily mean.

$$\alpha_{ET} = \ln\left(\frac{A}{ET_{coeff} \cdot K_S \cdot \tan\beta}\right) \quad (1)$$

This enhancement leads consequently to a more dynamic description of runoff formation, not only allowing for spatial changes in the location of the variable source-areas contributing to surface runoff but also creating a temporal course in the separation of runoff components. Saturation probability hence decreases during the growing season (when evapotranspiration rates are above the annual mean value) but increases in the winter months (Fig. 3).

Three soil storages, a soil root zone, an unsaturated zone and a saturated zone, regulate the distribution of water in the soil and, therefore, the partition of runoff into a surface and a sub-surface component (Fig. 4).

Thus, for each raster element and timestep *t,* the water availability in the soil root zone (SRZ) can be calculated by balancing the water content at *t*–1, the system input (rain, snowmelt) and the output (evapotranspiration) from the SRZ. Once the soil specific field capacity is reached, water is transferred from the SRZ to the unsaturated zone (SUZ), where the local storage deficit S_i can then be computed as a function of the mean storage deficit in the catchment S_m and the deviation of the local a_{ET} to its areal mean, γ, scaled by a recession parameter, *m,* (Eqn. 5).

$$S_i = S_m - m\left(\ln\frac{A}{ET_{coeff} \cdot K_S \cdot \tan\beta_i} - \gamma\right) \quad (2)$$

The parameterisation of the runoff model, including the calibration of the local saturated hydraulic conductivity K_s, which remains the only model-inherent 'fitting' parameter for the description of runoff formation, has been transferred with no change from the findings of an earlier study (Ludwig and Mauser, 2000). K_s was spatially determined from the digital soil type map using literature data and a sub-catchment specific scaling parameter, which was determined from hydrograph analysis. The recession parameter m is derived for each sub-catchment from an analysis of numerous baseflow recession curves, assuming the *1/Q* transformation of an exponential transmissivity profile (Ambroise *et al*., 1996). The values for m and K_s are not adjusted on an event basis but remain steady for all calculations. All further fluxes, such as the recharge rate into the saturated zone q_v or the baseflow volume Q_b of each sub-catchment at each timestep are calculated using the equations described by Obled *et al.* (1994) or Beven *et al*. (1995).

Saturation excess occurs in cases where water availability exceeds the actual storage deficit. Infiltration excess is calculated using the Green-Ampt infiltration model. Infiltration and saturation excess undergo an overland flow

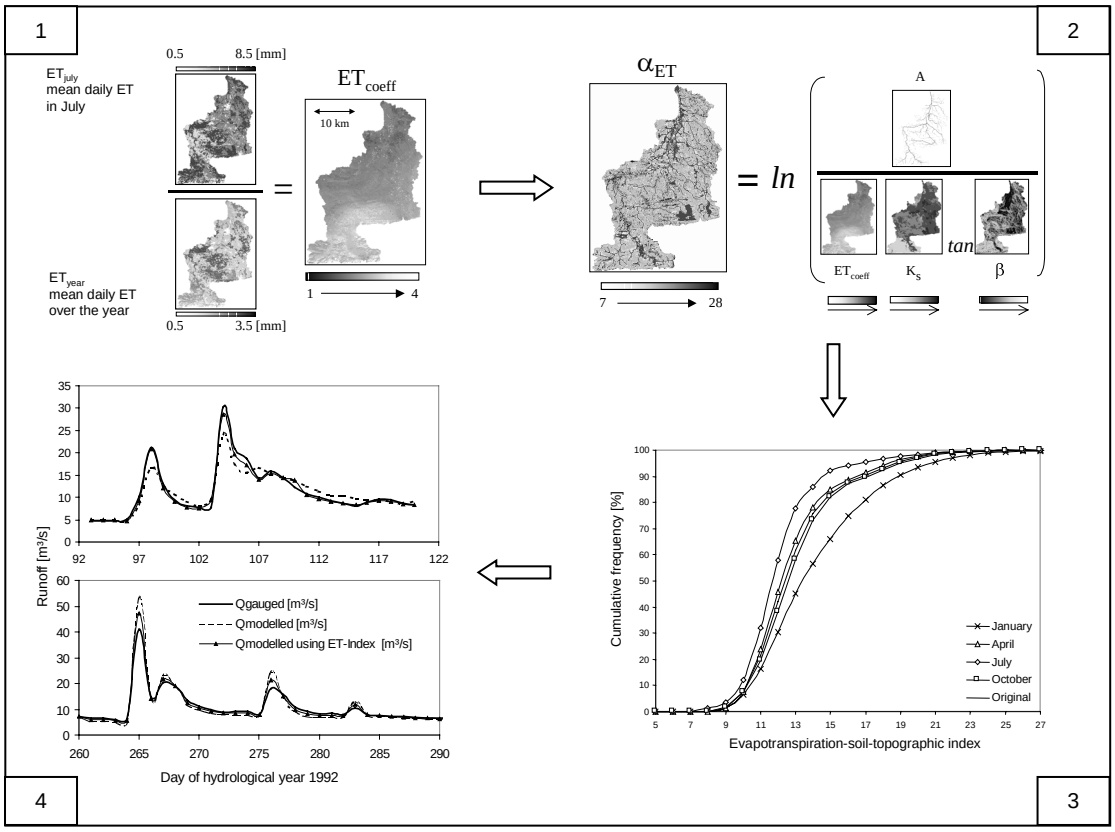

Fig. 3. *Mode of Operation of ET_c in the extended TOPMODEL concept (adapted from Ludwig and Mauser, 2000)*

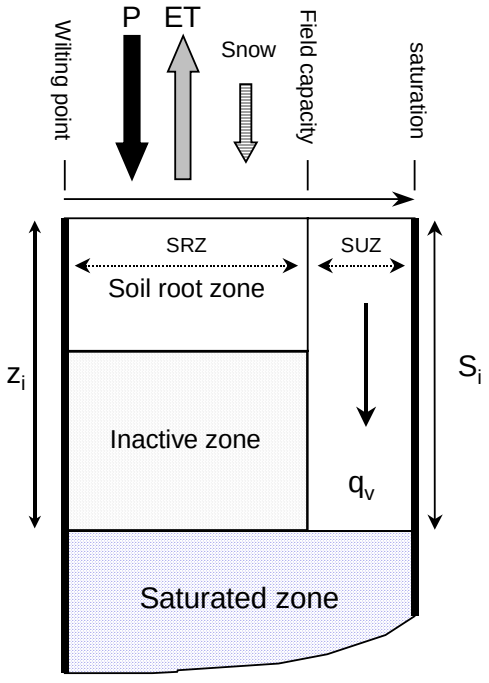

Fig. 4. *Soil water fluxes in TOPMODEL (based on Beven et al. 1995)*

algorithm based on the application of time-area functions, derived individually for each subcatchment from digital terrain analysis and field data using Manning's formula. Channel routing effects are considered using a simple approach based on an average flood wave velocity depending on the channel width in each reach length segment in relation to the actual outflow (derived from digital terrain analysis and water level recordings using the *Bankfull Discharge* method described by Allen *et al*., 1994)). Figure 5 summarises the setup of the linked meteorological-hydrological model framework

Processing of precipitation data

Hydrological simulations in the Ammer basin used three different precipitation inputs:

(a) surface observation data: (1) 12 DWD (German Weather Service) climatological stations with 3 measurements a day, (2) 10 DWD rain gauges sampled hourly;
(b) radar observations of precipitation provided by the DWD rain radar in Fuerholzen in a grid resolution of 1km by 1 km (sampled at a 1-hour time step);

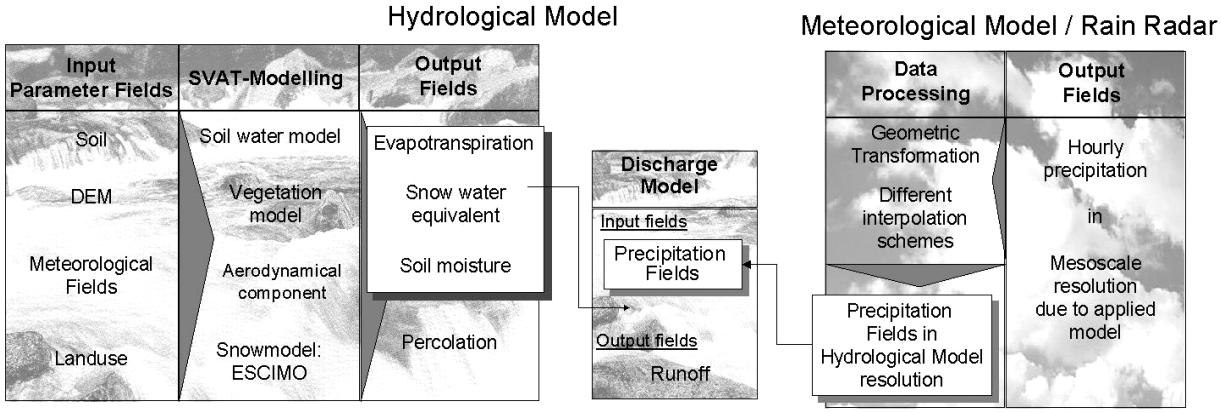

Fig. 5. *Model structure of the coupled hydrological and meteorological model*

(c) simulated precipitation fields of the following numerical weather prediction models in forecast mode (FC) and analysis mode (AN): SM (Swiss Model, Kaufmann *et al*., 2003), Meso-NH (Richard *et al*., 2003), BOLAM3 and MC2 (Benoit *et al*., 2003) in hourly time steps (for detailed descriptions of the NWP models, their background and theory, see the related special papers in this issue).

Since the hydrological model is applied on a 100 m grid and an hourly time step, all precipitation data have to be processed to these scales.

STATION MEASUREMENTS

The DWD climatic station measurements are recorded three times a day (7:30, 14:30, 21:30). To generate the meteorological input parameter fields for hourly modelling, these measurements have to be interpolated temporally and spatially. This is performed within the spatial modeller of PROMET. The temporal interpolation is performed using a spline function. Since precipitation is not continuous, a special algorithm is applied to distribute the measured rain for the timestep between the last two measurements. For shower events a Gaussian distribution is assumed; for continuous rainfall, the measured rain is distributed in equal parts. These data have then to be transformed from point measurements to a 100 m grid. After correcting the station measurements using a temperature and wind-speed dependent algorithm (Schulla, 1997), a linear regression trend analysis with elevation is performed, creating a timestep-specific trend level. The residuals of station measurements to this trend level are interpolated using a squared inverse distance function and are added to the formerly calculated trend level to reproduce the measured values.

DWD rain gauge measurements were made available as continuous analogue records. They were digitised and sampled to an hourly resolution. The spatial interpolation was carried out using a squared inverse distance algorithm. A combination of the two sets of recordings would usually be a suitable measure to counteract the problem of temporal and spatial interpolation errors. Due to the Ammer topography and the spatial distribution of the available stations, however, a cross-validation of interpolation results led to poor correspondence between the recorded data with no statistical significance. Therefore, the station data were treated and applied separately.

RAIN RADAR INTERPRETED PRECIPITATION

For one of the RAPHAEL flood events, rain radar interpreted precipitation from DWD weather radar in Fuerholzen was provided on a 1 km grid. The radar is located approximately 60 km north-east of the Ammer catchment. The data were corrected by the German Aerospace Center (DLR), accounting for beam blockage and non-standard drop size distribution. A simple disaggregation of equal distribution onto the 100 m model grid was performed. The temporal resolution of 1 hour was obtained by averaging aggregated 15 min intensities.

NWP PRECIPITATION DATA

Different new-generation mesoscale meteorological models were applied in the project, namely BOLAM3, MC2, Meso-NH and the Swiss Model, which provided an exemplary spectrum of the state-of-art in numerical weather prediction modelling. These models complement each other, since they differ not only in terms of dynamical and numerical aspects, but also in the respective parameterisation of physical atmospheric processes.

The data were provided at a 14 km resolution for the SM and at a 10 km resolution for the other models, over a time duration of 72 hours (time step: 1 hour). For one of the events described, Meso-NH and BOLAM3 provided information at a higher spatial resolution (2.5 and 3 km respectively) but for a shorter time period. After applying a uniform geometric projection, the meteorological model data were post-processed to meet the scale requirements of the hydrological model. They were downscaled to a 100 m grid by applying different interpolation schemes, such as simple disaggregation of the original resolution assuming a constant distribution over the pixel area, linear and a squared inverse distance interpolation (assuming that the meteo-model value represents the pixel centre) and disaggregation of data by distributing precipitation over a smoothed pixel-inherent surface, supposing that highest rainfall intensities occur at the highest elevation.

Model application

Within the RAPHAEL project, four Ammer flood events were selected as test periods for the coupled hydro/meteorological model approach, see Table 1. The test periods Ammer 1 and Ammer 2, have only limited coverage of NWP data; the meteorological origin, flood extent and finally the quality of the results are all in the range of the Ammer 3 event. The following test periods are described in detail: the Ammer 3 event (AM3, July 17th – 20th 1997), for which data were provided by all meteorological models in analysis and forecast mode, and the Ammer 4 event (AM4, May 20th – 23rd 1999), the most hazardous flood event ever recorded in the Ammer basin, for which also rain radar interpreted precipitation was available. These two events represent very different storms, in terms of both quantities and origin, and are therefore considered as suitable examples to interpret the effectiveness of the meteo-hydro model synergy.

THE AMMER 3 EVENT

Prior to the Whitsun flood in 1999, the period between July 17th and 20th 1997 has been selected as the Ammer flood event of highest priority within the project. Therefore, model results for all the meteorological models were made available by the project partner responsible in both analysis (AN) and forecast (FC) mode. Additionally, BOLAM3 and Meso-NH delivered data at higher spatial resolutions (HR) for a shorter time period (3 km and 2.5 km respectively, 36 hours). This summer event, in magnitude a bi-annual storm, was characterised by two distinct maxima, the first of approximately 150 $m^3 s^{-1}$ following a rather moderate filling of soil storages, and a second peak 18 hours later (~ 110 $m^3 s^{-1}$) caused by continued rainfall of rather low intensity.

Hydrological simulation results using station recordings

The DWD rain gauge measurements led to the most accurate hydrograph simulation (Fig. 6) except for a negative time shift of 1 hour and a slight underestimation of the second peak. With a peak difference of –1.5 % and an overall discharge volume underestimation of 10.8 %, the resulting coefficient of determination R^2 was 0.84.

The model calculation using the DWD climatic station measurements led to similar results. Showing a negative peak time shift of 3 hours, the shape of the hydrograph was approximated closely but the overall discharge volume was 7.1% low and the first peak was 4.5% low. Two possible error sources can be explored to interpret the modelled time shift. Because both results show the same trend, a connection to an incorrect temporal interpolation of precipitation data may explain the 'climatic stations' case (only three measured values per day are available). The other possibility is a malfunctional selection of routing parameters in the time-area-histograms of the runoff model. R^2 was 0.72.

Hydrological simulation results using NWP precipitation data

The results of applying the meteorological data in both the analysis and forecast mode showed a general inability to represent the first measured peak accurately. Comparing the simulated rates of precipitation with measured values explains this phenomenon as an extreme underestimation

Table 1. Availability of NWP model outputs and radar data for the RAPHAEL Ammer flood events

Event	*Date*	*SM*		*MC2*		*BOLAM3*			*MESO-NH*			*RADAR*
		FC	*AN*	*FC*	*AN*	*FC*	*AN*	*HR*	*FC*	*AN*	*HR*	
AM1	July 16 – 20, 1993	x	x	x	x		x			x		
AM2	Aug 27 – 31, 1995	x	x	x								
AM3	July 17 – 20, 1997	x	x	x	x	x	x	x	x	x	x	
AM4	May 20 – 23, 1999	x										x

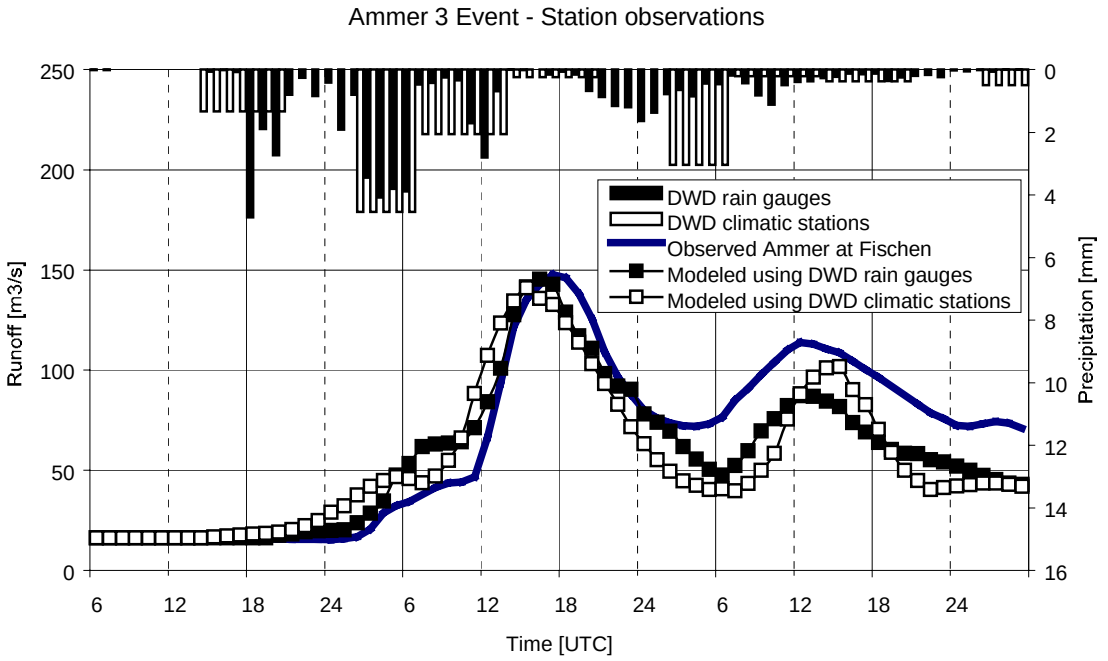

Fig. 6. *The hydrological model results of the Ammer 3 Event using station measurements*

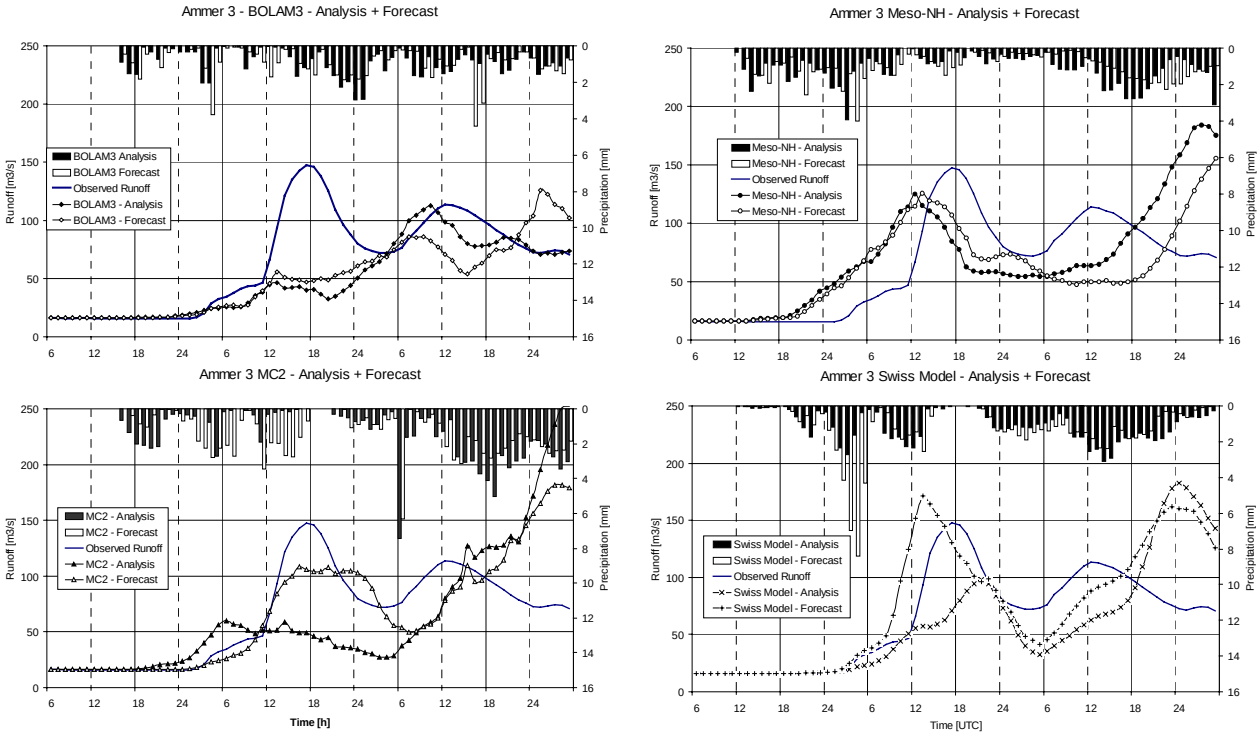

Fig. 7. *The hydrological model results of the Ammer 3 Event using NWP model data*

of rainfall amount (Fig. 7).

BOLAM3 completely missed the first peak (4 hours too early and –68.6% difference in peak discharge) but calculated the second one quite well (–2h). The concentration and recession of the modelled hydrograph was in reasonable agreement with the measured runoff. While the runoff volume was approximated closely (6%), R^2 is only 0.44, because of incorrect spatial and temporal distributions of rainfall patterns. The model run using forecasted data provided fairly similar results. Peak

discharge, overall discharge volume and predicted rainfall were comparable as were the associated time delays. The second peak was modelled less accurately. Due to a considerable change in areal rainfall distribution, the minimum relative runoff was over-emphasised and a delayed second peak was overestimated. R^2 was, therefore, only 0.39.

MC2 data provided results comparable to BOLAM3. The first peak was not generated due to a lack of precipitation at the beginning of the event. The peak discharge was underestimated by 60.2%. At the end of the event, high precipitation was predicted by MC2, leading to an enormous rise in the hydrograph, indicating a flood peak higher than the RAPHAEL flood window. Comparing the runoff volumes within the RAPHAEL time-frame led to a deviation of only –0.6 % but R^2 was only 0.12. In the forecast mode, MC2 showed a distinct first peak with a time shift of –1h and an underestimation of 26.7%. The second peak was lower than in the analysis mode but was still delayed and exceeded. The overall discharge volume had a surplus of 5.9% .

Meso-NH results differed considerably from those of BOLAM3 and MC2. The first peak was determined well, with a difference in peak discharge of only –15.4%. But the peak was 5 hours early, whereas the second peak was 15 hours later. The second flood wave was overestimated, because precipitation was assumed ongoing at the end of the event. Although the overall flood discharge volume was miscalculated by only 10%, the value of R^2 reached only 0.21. The modelled hydrograph using the Meso-NH forecast mode precipitation deviated only marginally from the analysis mode application. The overall flood discharge volume was miscalculated by –2.6%, with an additional increase in the peak time delay.

The Swiss Model (SM) result was similar to Meso-NH. While the starting point of surface runoff was met accurately, the first peak was underestimated by 33.7% along with a time displacement of 4 hours. As in Meso-NH and MC2, the second peak was much higher with a time shift of 12 hours. The overall flood volume was underestimated by –7.5%, and R^2 was only 0.29. The largest deviations between analysis mode and forecast mode occurred for the Swiss model data sets. The rise of the hydrograph was calculated fairly accurately, but the first distinct peak was four hours early and was overestimated by 16.1%. The second peak was still late and overestimated. However, in comparison with the analysis mode, the second peak was smaller, which is also apparent for the MC2 and the Meso-NH data set.

Among the meteorological model data sets, the largest value of the coefficient of determination ($R^2 = 0.56$) for the Ammer 3 event was achieved using the Swiss model forecast mode.

High resolution NWP model data were made available from BOLAM3 and Meso-NH, with Meso-NH additionally providing a data set derived from a model run implementing an ice-phase algorithm. The NWP data covered only the starting hours of the Ammer 3 event but, nevertheless, are indicative of the modelled accuracy of the initial conditions for the flood event. Compared to the standard resolution mode, BOLAM3 surprisingly inverted the starting conditions and modelled a remarkable surplus of precipitation, so that modelled runoff was overestimated. Meso-NH predicts a very similar temporal distribution of rainfall, with the corresponding hydrograph of even higher magnitude. Much better agreement with measurements was achieved using the Meso-NH ice-phase data. Although the modelled runoff was again over-estimated, the overall

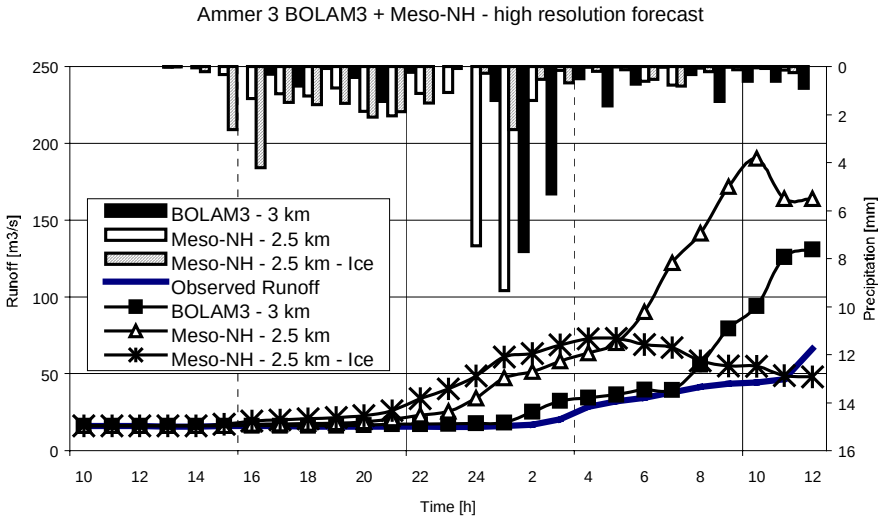

Fig. 8. *The hydrological model results of the Ammer 3 Event –High resolution Forecast mode (BOLAM3 and Meso-NH only)*

amount of rainfall was far less than that predicted in the high-resolution standard mode (Fig. 8).

THE AMMER 4 EVENT ('WHITSUN FLOOD')

The most hazardous flood ever recorded in the Ammer catchment occurred during the RAPHAEL project, and is referred to as the 1999 'Whitsun flood'.

An unusually steady advective rainband across Southern Germany caused a 48-hour period of excessive rainfall north of the Alps; this resulted in the highest daily rainfall amount ever recorded in the Ammer catchment (138.7 mm at the gauge at Hohenpeissenberg on 21st May). The rainfall during the event induced snow melting at higher altitudes (~ 1800m asl). On account of the preceding precipitation and snowmelt, soils were mostly saturated and, thus, almost all precipitation and melt water was transformed to direct runoff. The consequent floods in Southern Bavaria were hazardous and caused extensive damage. The water level stages recorded along the Ammer correspond to a bicentennial flood.

Comparison of available precipitation data

As precipitation data inputs, a 96-hour forecast of the Swiss Model (SM), rain radar data from the DWD Fuerholzen Radar and recordings from DWDs gauging stations were available.

In a first step, a pixel-wise analysis of precipitation data was performed, comparing rainfall intensities extracted from the various data sources to the measurements of the raingauge at Weilheim for a 96h-period (Fig. 9). SM results, initialised by the boundary conditions of DWD's Europa Model, are downscaled to a 100 m grid by applying three different interpolation schemes: standard disaggregation by equal distribution (SM-multiplied), linear interpolation assuming that the modelled rainfall represents the centre of the 14 km pixel (SM-interpolated) and a quadratic inverse distance algorithm (SM-disaggregated). Rain radar-interpreted precipitation is disaggregated by means of equal distribution.

Reasonable agreement can be detected in the temporal sequence but the intensities vary considerably depending on the chosen data set and disaggregation scheme. Table 2 shows the statistics of the pixel-wise data comparison. R^2 and the Root Mean Square Error (RMSE) are used as the objective functions to describe the data correlation.

Some significant features can be detected in Fig.9. Although agreement with measurements was good for the NWP data, precipitation was overestimated at the beginning

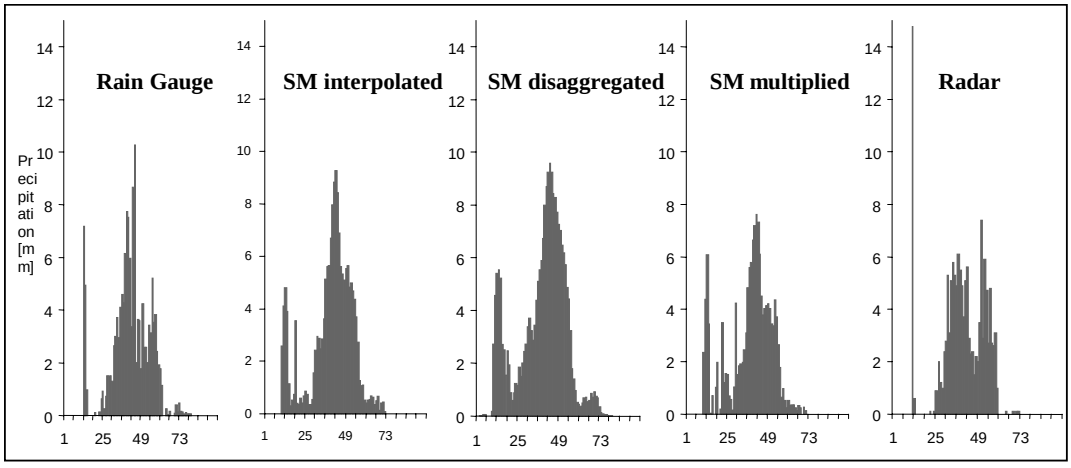

Fig. 9. *Point comparison of measured to modelled precipitation data at Weilheim gauge (taken from Taschner et al., 2001)*

Table 2. Statistics of point precipitation at gauge Weilheim for the Whitsun Flood

	Recorded precipitation at Weilheim Σ = 147.5 mm			
	SM-disaggregate	*SM-interpolated*	*SM-multiplied*	*DWD Rain Radar*
R^2	0.69	0.64	0.65	0.28
RMSE (mm)	1.40	1.96	1.37	2.28
Σ (mm)	172.2	222.4	147.9	142.2

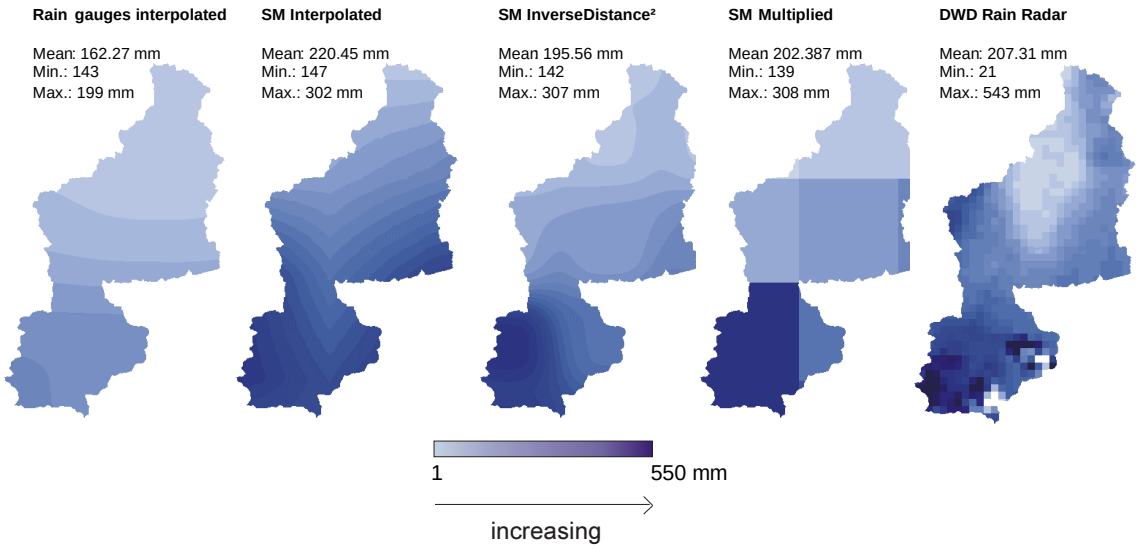

Fig. 10. *Accumulated areal precipitation in the Ammer catchment for the Whitsun Flood*

Table 3. Statistics of areal precipitation for the Whitsun Flood

	Mean [mm]	*Min [mm]*	*Max. [mm]*
Rain gauge	162	143	199
SM multiplied	202	139	308
SM interpolated	220	147	302
SM disaggregated	195	142	307
Rain Radar	207	21	543

of the event; this led to an unrealistic filling of the soil storage and, hence, a reduction in its storage capacity, resulting in a quicker catchment response of surface runoff. Radar data has the worst correlation ($R^2 = 0.28$) with measurements and shows a second distinct rainfall maximum towards the end of the event, which is not present in any other data source.

Secondly, the spatial distribution of the 96-h aggregated precipitation is compared (Fig. 10, Table 3). While the images show a positive southbound gradient of areal precipitation, there are remarkable differences in its intensity. Distinct maxima of rainfall amount in the south-western part of the catchment are provided by both NWP model and rain radar. In comparison with measurements, NWP model and rain radar deliver significantly higher areal means; in particular, the maximum values drastically exceed the measured values. The rain radar variance is extremely high, perhaps because of the effects of ground clutter and beam blockage at the alpine ridges.

Hydrological simulation results for the Whitsun flood

The runoff modelled using interpolated rain gauge data again delivered a good approximation of the recorded hydrograph. Results refer to the stream-gauge at Weilheim ($R^2 = 0.91$), because lake ponding affected the recordings at the Fischen gauge. The integrated 96 h runoff volume was underestimated by only 9%, while the simulated peak discharge was 12% low. It has to be kept in mind that, because of dam breaks along the Ammer, a higher actual runoff volume and peak has to be assumed (Fig. 11).

The model runs applying the SM results show general overestimations of runoff volume (15% (SM-disaggregated), 27% (SM-multiplied), 46% (SM-interpolated)) and peak discharge (30% (SM-disaggregated), 35% (SM-multiplied), 67% (SM-interpolated)) with a corresponding time displacement of one to three hours. The overestimation of runoff simulated using SM data can be attributed to an overestimation of precipitation for 20 May 1999, leading to an unrealistic decrease in soil water deficits in advance of the flood event. These divergent initial conditions resulted in an early rise and a general surplus of modelled flood discharge. The temporarily delayed maximum in discharge simulated using the rain radar data was caused by an extreme overestimation of precipitation in the southernmost alpine region, because of ground-clutter corrections. The coefficients of determination comparing the modelled discharge with the recordings were 0.61 for the rain radar and 0.83 for the SM rainfields. Table 4 is a statistical summary of the results of coupled modelling for the test cases presented in the Ammer catchment.

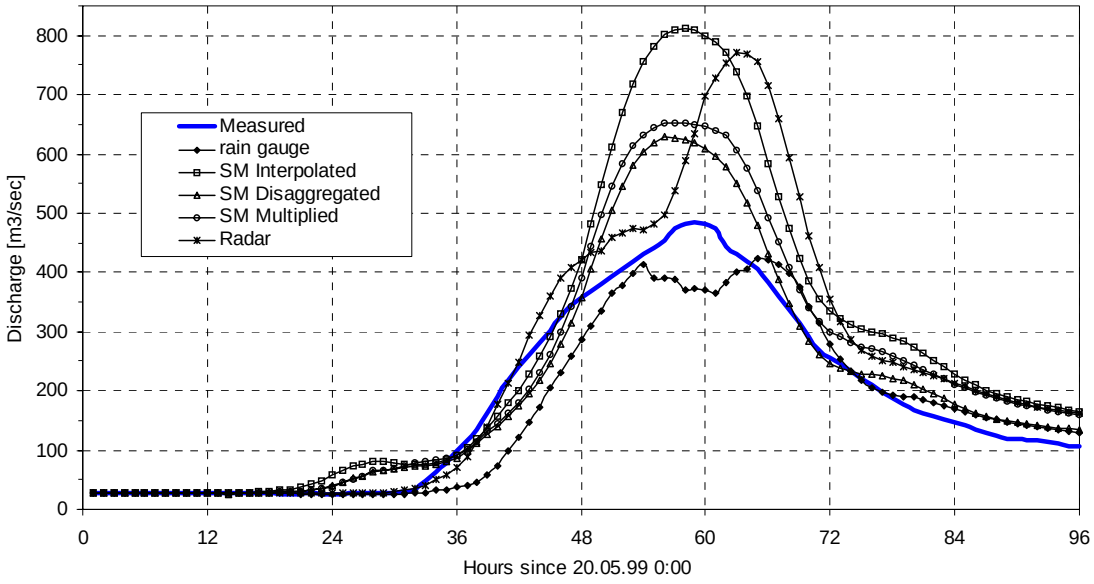

Fig. 11. *The hydrological model results of the Ammer 4 Event (May 20th – 23rd 1999)*

Table 4. Multi-scenario hydrograph statistics for the Whitsun Flood

Deviation to measured runoff	*Peak flow [%]*	*Runoff volume [%]*	*Peak Time [h]*	R^2
Rain gauge	–9	–13	–6, + 6	0.89
SM multiplied	+ 25	+ 27	–2	0.82
SM disaggregated	+ 21	+ 15	–3	0.83
SM interpolated	+ 57	+ 36	–1	0.66
Rain Radar	+ 51	+ 20	+ 8	0.61

Sensitivity analysis of the coupled hydro-meteorological model approach

A method to provide an uncertainty estimation is applied, performing a radial shift of the spatial domain modelled by the SM. Simulated rainfields were moved by one-pixel (14 km) in each direction, showing tremendous deviations in terms of precipitation volume and temporal distribution. The spatial distribution of aggregated shifted rainfall showed, for the southern rain-fields (i.e. a northbound shift), an increase in precipitation over the whole catchment area, while northern rain fields approximated the interpolated rain gauge derived precipitation field rather better. The best agreement in terms of precipitation amount compared to measurements was achieved using the north-western rain field (162.27 mm measured versus 160.12 mm modelled NW).

This is also reflected in the simulated hydrographs (Fig. 12). An obvious overestimation of the flood is modelled applying the southern rainfields. Shifting the rainfield to the east and west produces hydrographs fairly similar to the original data. The use of the southbound shifted rainfield (referred to as 'North' in Fig. 12) shows the best correspondence between modelled and measured runoff (R^2 = 0.96, RMSE = 37.97 $m^3 s^{-1}$). This procedure of rainfield shifting may be used to provide flood forecasting information automatically within a certain range of reliability, defining the minimum and maximum boundary values of possible predictions.

Discussion and conclusions

The major scope of the RAPHAEL project was to assess the possibilities for improved flood forecasting in complex mountain catchments using one-way coupled meteo-hydrological model set-ups. The combination of NWP models and the hydrological model PROMET-D for flood analysis in the Ammer catchment shows the promising capacity of this synergistic approach. However, some problems emerged from the analyses.

Conventional rain gauging is inaccurate on account of several well-known but barely quantifiable error-sources, such as wind turbulence, evapotranspiration or wetting. Correction-algorithms can counteract these systematic errors only by using empirically determined coefficients, which are generally not transferable in time and space.

Rain radars provide images of spatially distributed rainfall

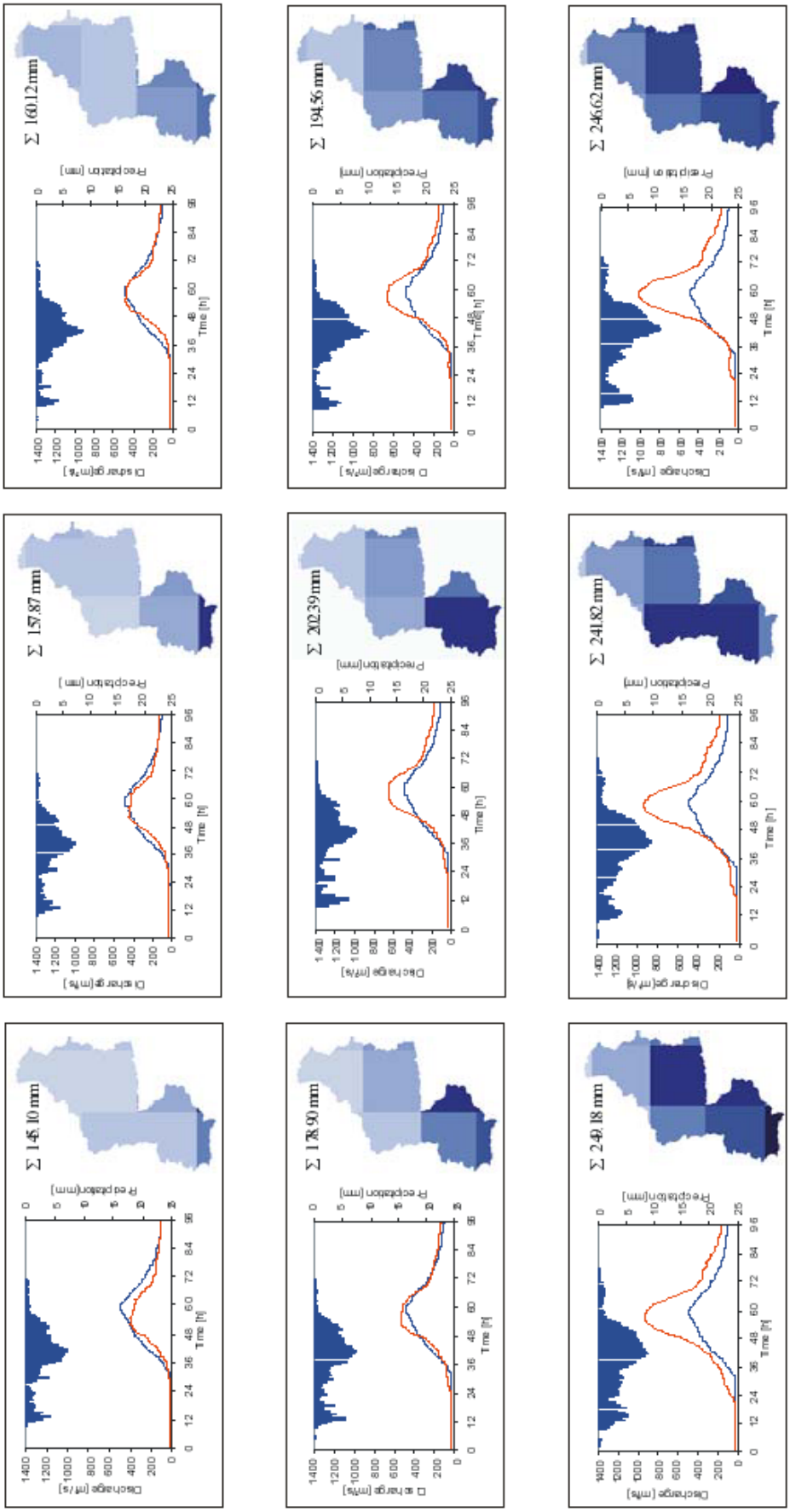

Fig. 12. *Hydrological model results using a radial NWP rainfield shifting method (adapted from Taschner et al., 2001)*

intensities at a high temporal and at reasonable spatial resolution. However, these intensities are provided at coarse intervals, due to high uncertainties in the available reflectivity equations. Exact knowledge of the actual drop size distribution or even the phase of precipitation is generally not available and, hence, requires complex, but still uncertain, correction procedures. In the application presented, several problems arise from attenuation effects because the radar is up to 80 km away and beam blockages occur at the alpine ridges.

Mesoscale meteorological models are basically the only data source to provide rainfall forecasts over large areas with high temporal resolution. When applying the models to a large domain over the Alps, significant similarities in spatial distribution and precipitation volume can be identified. Internal deviations refer to the boundary conditions applied in macroscale models, such as the Europa Modell of the German Weather Service or the ECMWF, which work at even larger scales.

The different simulations in this study prove, in principle, the capacity of NWP models to describe meteorological patterns for accumulated periods accurately. However, the very coarse spatial resolution (10 – 14 km) is a disadvantage for hydrological catchment applications; disaggregating and downscaling of data are necessary and, hence, an additional potential error source is introduced. Even minor deviations in NWP results can then be crucial for flood modelling at the catchment scale. When the high resolution structures of rainfields in complex convective meteorological situations cannot be represented accurately in time and space, it leads to uncertainty in the basin-wide availability of water for flood generation and hence in flood simulations. Furthermore, the complex physics, simulated in the meteorological models, requires sophisticated algorithms and high computer power, which few institutions are able to provide.

The selected Ammer events show that, at the current stage of research, a high variability in flood modelling results still has to be accepted; this leads to the conclusion that the probability for reliable flood forecasting based on NWP model outputs is presently low. Nevertheless, as demonstrated for the Whitsun Flood in 1999, good results can be obtained under certain circumstances, i.e. foreseeable and stable meteorological situations.

While current hydrological models have reached acceptable accuracy in flood modelling, meteorological models do not yet meet the requirements of microscale catchment applications. The hydrological community is responsible for achieving a better understanding of the parameters influencing the rainfall patterns within a mesoscale NWP model pixel, for which more advanced disaggregation and downscaling methods will be necessary.

An integrated assemblage of rain gauges connected on-line, rain radar measurements and remotely sensed data within meteorological models will be an important advance in obtaining more accurate rainfall prediction. Coupled meteo-hydro models will then serve as a useful tool for flood-warning services.

Acknowledgements

Research for this study was funded within the EU-project RAPHAEL (ENV4-CT97-0052). The valuable contributions of all RAPHAEL partners are gratefully acknowledged. The meteorological data were generously supplied by the DWD. The Bavarian Water Authority kindly providied the stream gauge measurements. Special thanks go to Keith Beven for sharing the basic TOPMODEL codes and to Jurgen Garbrecht for providing the TOPAZ software package.

References

Allen, P.M., Arnold, J.G. and Byars, B.W., 1994. Downstream Channel Geometry for Use in Planning-Level Models. *Water Resour. Bull.*, **30**, 663–671.

Ambroise, B., Beven, K.J. and Freer, J., 1996. Towards a generalisation of the TOPMODEL concepts: topographic indices of hydrological similarity, *Water Resour. Res.*, **32**, 2135–2145.

Bacchi, B. and Ranzi, R., 2003. The RAPHAEL project: An Overview. *Hydrol. Earth Syst. Sci.*, **7**, 784–798.

Baldocchi, D.D., Hicks, B.B. and Camara, P., 1987. A canopy stomatal resistance model for gaseous depositions to vegetated surfaces. *Atmos. Environ.,* **21**, 91–101.

Benoit, R., Yu, W., Chamberland, S., Pellerin, P. and Kouwen, N., 2003. Hydrometeorological aspects of the Real-Time Ultrafinescale Forecast Support during the Special Observing Period of the MAP. *Hydrol. Earth Syst. Sci.*, **7**, 877–889.

Beven, K.J. and Kirkby, M.J., 1979. A physically based variable contributing area model of basin hydrology. *Hydrolog. Sci. Bull.*, **24**, 43–69.

Beven, K.J. and Wood, E.F., 1983. Catchment geomorphology and the dynamics of runoff contributing areas. *J. Hydrol.*, **65**, 139–158.

Beven, K.J. and Wood, E.F., 1993. Flow routing and the hydrological response of channel networks. Chapter 5 of *Channel Network Hydrology*, K.J. Beven and M.J. Kirkby (Eds.). Wiley, Chichester, UK.

Beven, K.J., Lamb, R., Quinn, P.F., Romanowicz, R. and Freer, J., 1995. TOPMODEL. In: *Computer Models of Watershed Hydrology*, V. P. Singh (Ed.). Water Resources Publications. 627–668.

Brooks, R.H. and Corey, A.T., 1964. Properties of porous media affecting fluid flow. *J.. Irrig. Drain. Div.*, Amer. Soc. Civil Eng. IR2, 61–88.

Eagleson, P.S., 1978. Climate, soil and vegetation, 1–7. *Water Resour. Res.*, **14**, 705–776.

Franchini, M., Wendling, J., Obled, C. and Todini, E., 1996. Physical interpretation and sensitivity analysis of the TOPMODEL. *J. Hydrol.*, **175**, 293–338.

Garbrecht, J. and Martz, L., 1995. *TOPAZ - Version 1.1*. National Agricultural Water Quality Laboratory, USDA, Agricultural Research Service, Durant, Oklahoma, USA.

Kaufmann, P. Schubiger, F. and Binder, P., 2003. Precipitation forecasting by a mesoscale NWP model: eight years of experience. *Hydrol. Earth Syst. Sci*., **7**, 812–832.

La Barbera, P., Lanza, L.G. and Stagi, L., 2002. Tipping bucket mechanical errors and their influence on rainfall statistics and extremes. *Water Sci. Technol*., **45**, 1–9.

Lombardo, F. and Stagi, L., 1997. Dynamic calibration of rain gauges in order to check errors due to heavy rain rates. *Proc. Int. Conf.* '*Water in the Mediterranean*', Istanbul, 25–29 November.

Ludwig, R. and Mauser, W., 2000. Modelling catchment hydrology within a GIS-based SVAT model framework. *Hydrol. Earth Syst. Sci.*, **4**, 239–249.

Mauser, W., 1989. *Die Verwendung hochauflösender Satellitendaten in einem Geographischen Informationssystem zur Modellierung von Flächenverdunstung und Bodenfeuchte.* Habilitationsschrift, Albert-Ludwigs-Universität, Freiburg i.Br.

Mauser, W. and Schädlich, S., 1998. Modelling the spatial distribution of evapotranspiration on different scales using remote sensing data. *J. Hydrol*., **212/213**, 250–267.

Monteith, J., 1978. Evaporation and the environment. *Symp. Soc. Expl. Biol.,* **19**, 205–234.

Norman, J.M., 1979. *Modelling the complete plant canopy. Modification of the Areal Environment of Plants*. Amer. Soc. Agric. Eng. St. Joseph, USA. 249–277.

Obled, Ch., Wendling, J. and Beven, K.J., 1994. The sensitivity of hydrological models to spatial rainfall patterns: an evaluation using observed data. *J. Hydrol.*, **159**, 305–333.

Philip, J.R., 1957. The theory of infiltration: 1. The infiltration equation and its solution. *Soil Sci*., **83**, 345–357.

Richard, E., Cosma, S., Benoit, R., Binder, P. and Buzzi, A., 2003. Intercomparison of mesoscale meteorological models for weather forecasting. *Hydrol. Earth Syst. Sci*., **7**, 799–811.

Schulla, J., 1997. Hydrologische Modellierung von Flußgebieten zur Abschätzung der Folgen von Klimaänderungen. *Züricher Geographische Schriften*, H. 69, 161 S., Zürich, Switzerland.

Sevruk, B. (Ed.)., 1986. Correction of precipitation measurements. *Zürcher Geographische Schriften*, **23**. 288pp., Zürich

Strasser, U. and Mauser, W., 2001. Modelling the spatial and temporal variations of the water balance for the Weser catchment 1965-1994. *J. Hydrol*., **254**, 199–214.

Stolz, R., Strasser, G. and Mauser, W., 1999. A knowledge based multisensoral and multitemporal approach for land use classification in rugged terrain using LANDSAT-TM and ERS SAR. *Proc. SPIE*, **3868**, 195–206.

Taschner, S., Ludwig, R. and Mauser, W., 2001. Flood modelling in a mountain watershed using inputs from rain-radar and mesoscale meteorological models. *IAHS Publication no. 267*, 586–588.

Todini, E., 1996. The ARNO rainfall-runoff model. *J. Hydrol.,* **175**, 339–382.